ORIGINAL ARTICLE – CANCER RESEARCH

The PI3K pathway impacts stem gene expression in a set of glioblastoma cell lines

Eduardo Martinez[1] · Neftali Vazquez[1] · Alma Lopez[1] · Victor Fanniel[1] · Lilia Sanchez[1] · Rebecca Marks[1] · Leetoria Hinojosa[1] · Victoria Cuello[1] · Marisa Cuevas[1] · Angelica Rodriguez[1] · Cerin Tomson[1] · Andrea Salinas[1] · Mark Abad[1] · Martin Holguin[1] · Noel Garza[1] · Abraham Arenas[1] · Kevin Abraham[1] · Luis Maldonado[1] · Vivian Rojas[1] · Alex Basdeo[1] · Erin Schuenzel[1] · Michael Persans[1] · Wendy Innis-Whitehouse[2] · Megan Keniry[1]

Abstract

Background The PI3K pathway controls diverse cellular processes including growth, survival, metabolism, and apoptosis. Nuclear FOXO factors were observed in cancers that harbor constitutively active PI3K pathway output and stem signatures. FOXO1 and FOXO3 were previously published to induce stem genes such as *OCT4* in embryonic stem cells. Here, we investigated FOXO-driven stem gene expression in U87MG glioblastoma cells.

Methods PI3K-activated cancer cell lines were investigated for changes in gene expression, signal transduction, and clonogenicity under conditions with *FOXO3* disruption or exogenous expression. The impact of PI3K pathway inhibition on stem gene expression was examined in a set of glioblastoma cell lines.

Results We found that CRISPR-Cas9-mediated *FOXO3* disruption in U87MG cells caused decreased *OCT4* and *SOX2* gene expression, STAT3 phosphorylation on tyrosine 705 and clonogenicity. *FOXO3* over expression led to increased *OCT4* in numerous glioblastoma cancer cell lines. Strikingly, treatment of glioblastoma cells with NVP-BEZ235 (a dual inhibitor of PI3K and mTOR), which activates FOXO factors, led to robust increases *OCT4* gene expression. Direct FOXO factor recruitment to the *OCT4* promoter was detected by chromatin immunoprecipitation analyses using U87MG extracts.

Discussion We show for the first time that FOXO transcription factors promote stem gene expression glioblastoma cells. Treatment with PI3K inhibitor NVP-BEZ235 led to dramatic increases in stem genes in a set of glioblastoma cell lines.

Conclusion Given that, PI3K inhibitors are actively investigated as targeted cancer therapies, the FOXO-mediated induction of stem genes observed in this study highlights a potential hazard to PI3K inhibition. Understanding the molecular underpinnings of stem signatures in cancer will allow refinements to therapeutic strategies. Targeting FOXO factors to reduce stem cell characteristics in concert with PI3K inhibition may prove therapeutically efficacious.

Keywords FOXO transcription factors · Stem genes · *OCT4* · PI3K inhibition · Glioblastoma

Abbreviations

PI3K	Phosphatidylinositol 3 Kinase
PIP2	Phosphatidylinositol 4,5-bisphosphate
PIP3	Phosphatidylinositol 3,4,5-trisphosphate
AKT	Protein Kinase B
PTEN	*Phosphatase and Tensin homolog deleted on chromosome ten*
FOXO	Forkhead box subfamily O
ES	Embryonic stem
GBM	Glioblastoma multiforme
BBC	Basal breast cancer
OCT4	*Octamer-binding Transcription factor 4*
SOX2	*Sex determining region Y-box 2*
CRISPR	Clustered Regularly Interspaced Short Palindromic Repeats
Cas9	CRISPR-associated sequence 9

✉ Megan Keniry
megan.keniry@utrgv.edu

1 Department of Biology, University of Texas-Rio Grande Valley, 1201 W. University Dr., Room: ESCNE 4.633, Edinburg, TX 78539, USA

2 School of Medicine, University of Texas-Rio Grande Valley, 1201 W. University Dr., Edinburg, TX 78539, USA

NPTII	Neomycin resistance cassette (*Neomycin phosphotransferase*)
ATCC	American Type Culture Collection
MEM	Minimal essential media
DMEM	Dulbecco's Modified Eagle Medium
RPMI	Roswell Park Memorial Institute (*RPMI*) 1640 Medium
FBS	Fetal bovine serum
PBS	Phosphate-buffered saline
SDS-PAGE	Sodium dodecyl sulfate-polyacrylamide gel electrophoresis
PVDF	Polyvinylidene fluoride
TBST	1X Tris-buffered saline with Tween 20
kDa	Kilo Dalton
ACTB	Beta actin
LIF	*Leukemia Inhibitory Factor*
IL6	*Interleukin 6*
NANOG	*Nanog homeobox*
SHH	*Sonic Hedge Hog*
TGFB1	*Transforming Growth Factor beta1*
EGF	*Epidermal Growth Factor*
ALPP	*Alkaline Phosphatase Placental*
TUBB3	*Tubulin Beta 3 class III*
STAT3	Signal transducer and activator of transcription 3
JAK2	Janus Kinase 2
IBC	Institutional Biosafety Committee
Cyt	Cytoplasm
Nuc	Nucleus

Introduction

The Phosphatidylinositol-3 Kinase (PI3K) pathway is evolutionarily conserved and plays crucial roles in survival, growth, cell cycle, and metabolism (Luo et al. 2003; Manning and Cantley 2007; Nakae et al. 2001; Okkenhaug and Vanhaesebroeck 2003). PI3K phosphorylates phosphatidylinositol 4,5-bisphosphate (PIP$_2$) producing phosphatidylinositol 3,4,5-trisphosphate (PIP$_3$), which binds to and activates targets such as serine threonine kinase AKT (Bellacosa et al. 1998; Manning and Cantley 2007). AKT has over 20 identified substrates including the transcription factors Forkhead Box subfamily O members (FOXO-1, -3, and -4) (Brunet et al. 1999; Luo et al. 2003; Manning and Cantley 2007). Phosphorylation of FOXO factors by AKT leads to their cytoplasmic sequestration/inactivation (Brunet et al. 1999).

The PI3K pathway is almost universally activated in cancer to promote growth and survival, commonly by gain-of-function *PIK3CA* mutants (encoding PI3K catalytic subunit) or loss-of-function *PTEN* (*Phosphatase and Tensin homolog deleted on chromosome ten*) mutations (Li et al. 1997; Saal

et al. 2005, 2007, 2008). Aberrant activation of the PI3K Pathway leads to inactivation of FOXO transcription factors (Brunet et al. 1999). However, several studies have shown exceptions to this canonical PI3K Pathway circuitry in certain advanced poor prognosis cancers, human embryonic stem (ES) cells, and naïve T cells (Bigarella et al. 2017; Keniry et al. 2013; Oh et al. 2012; Trinh et al. 2013). In these settings, PI3K expression is high, but a portion of the FOXO proteins is found in the nucleus (Keniry et al. 2013; Liang et al. 2016; Oh et al. 2012; Zhang et al. 2011). FOXO1 and FOXO3 are required for the maintenance of hematopoietic, embryonic, and neural stem cells (Miyamoto et al. 2007; Renault et al. 2009; Tothova and Gilliland 2007; Tothova et al. 2007; Yu et al. 2018; Zhang et al. 2011). In ES cells, FOXO1 directly associated with the promoters and regulated *Octamer-binding Transcription factor 4* (*OCT4*) and *Sex determining region Y-box 2* (*SOX2*), thereby promoting pluripotency and preventing differentiation (Zhang et al. 2011). Given that FOXO factors regulate *OCT4* in stem cells, we examined whether these factors had a similar function in certain cancers (Ben-Porath et al. 2008; Ghaffari et al. 2010).

Forkhead Box O (FOXO-1, -3, and -4) transcription factors regulate cellular processes in a context-dependent manner and are partially redundant with each other (Paik et al. 2007; Tothova et al. 2007). FOXO6 is mainly expressed in the brain and regulated by distinct mechanisms (Jacobs et al. 2003; van der Heide et al. 2005). FOXO-1, -3, and -4 are excluded from the nucleus in settings with high PI3K output (via an AKT-mediated mechanism) (Brunet et al. 1999). There are a number of settings in which FOXO factors at least partially bypass AKT regulation, leading to nuclear localization (Keniry et al. 2013; Liang et al. 2016). First, *FOXO1* was found mutated in 9% of diffuse large B-cell lymphoma (DLBCL) leading to constitutive nuclear localization; these mutations were associated with poor prognosis (Trinh et al. 2013). Nuclear FOXO factors were also found in basal breast cancer (BBC) cell lines such as BT549 as well as primary samples that harbored active PI3K Pathway output (Hagenbuchner et al. 2016; Keniry et al. 2013; Zhang et al. 2011). However, the function of nuclear FOXO factors in these aggressive cancers with active PI3K pathway output remained elusive.

To gain insight into novel roles for FOXO factors in aggressive poor prognosis cancers, we built genetic models using CRISPR Cas9 genome editing technology (Vazquez et al. 2018). We specifically disrupted the *FOXO3* gene with a neomycin resistance cassette (*NPTII*) producing a truncation mutant in glioblastoma (GBM) U87MG cells (Vazquez et al. 2018). Using this genetic model, we examined known FOXO target genes (identified in ES cells) for differential expression. We found significantly decreased expression of stem genes such as *OCT4* and *SOX2* in the *foxo3* mutant

U87MG cells compared to parental U87MG control cells (Figs. 1, 2). Subsequent experiments revealed that FOXO3 more broadly promoted stem gene expression and signal transduction (Figs. 2, 3). Inhibition of the PI3K pathway with NVP-BEZ235 led to dramatically increased expression of stem markers *OCT4* and *ALPP* (encoding alkaline phosphatase*)*, at least in part, via an FOXO-dependent mechanism. These results suggest a potential hazard for clinical use of PI3K inhibition as a therapeutic (especially in cancers that harbor stem signatures), (Figs. 3, 4). Taken together, our findings highlight a novel role for FOXO factors in cancer, which is to promote stem programs that likely contribute to aggressiveness.

Results

CRISPR Cas9-mediated *FOXO3* disruption reduced *OCT4* gene expression in U87MG cells

Poor-prognosis cancers such as GBM and BBC harbor stem cell signatures, including expression of genes *OCT4* and *SOX2*, but the mechanisms that induce these programs remain to be fully elucidated (Ben-Porath et al. 2008). Given that FOXO factors induce *OCT4* and *SOX2* genes in human and mouse ES cells, we examined the expression of these putative targets in GBM cells that harbor nuclear FOXO (Zhang et al. 2011). In our previous work, we built genetic models using CRISPR Cas9 genome editing to disrupt the *FOXO3* gene in U87MG GBM cells with a neomycin resistance cassette (Vazquez et al. 2018). The foxo3 truncation mutant protein retained the DNA-binding domain, but lacked the trans-activation domain and was approximately 45 kDa compared to the 80 kDa full-length protein
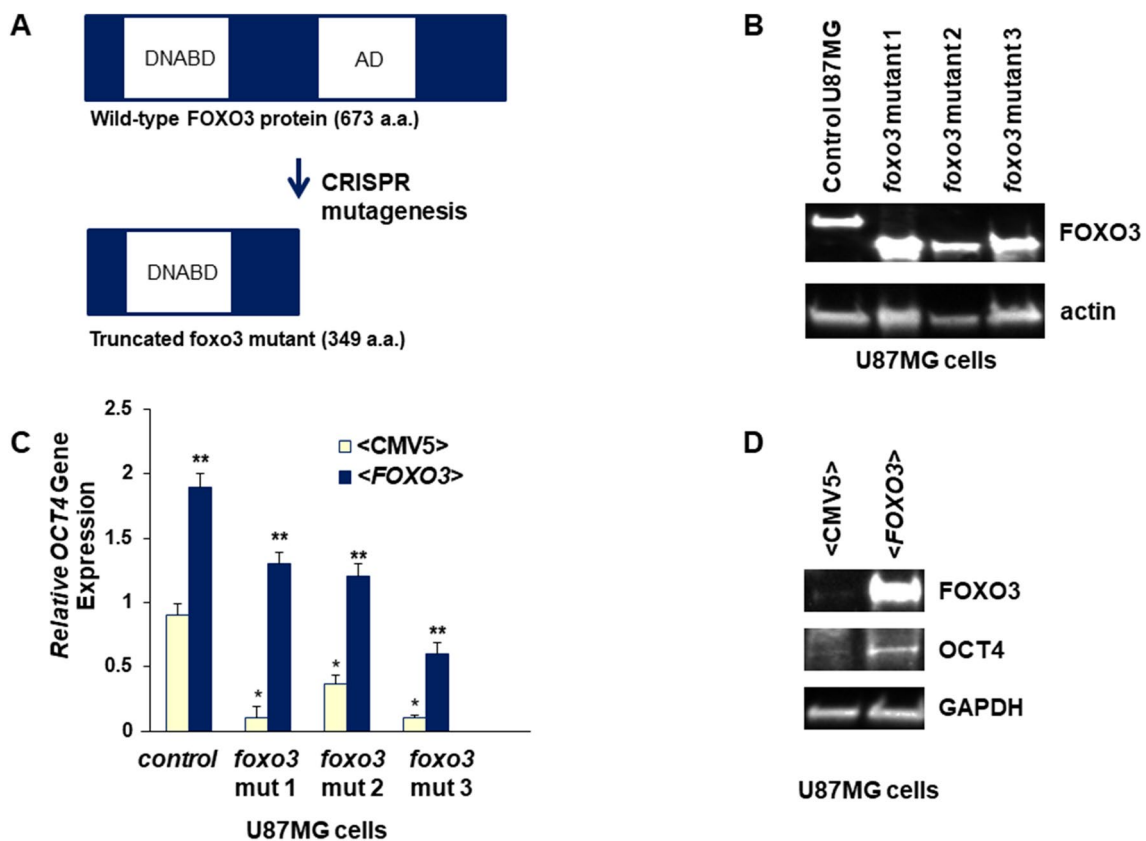

Fig. 1 *FOXO3* impacts *OCT4* Gene Expression. **a** Schematic of foxo3 disruption mutant protein (DNABD = DNA Binding Domain) and AD = transcriptional activation domain). **b** Total protein lysates prepared from *foxo3* mutant containing U87MG cells and control cells were examined by western blot analysis; antibodies used for western blotting are indicated. Wild-type FOXO3 was approximately 80 kDa, whereas mutant foxo3 protein was approximately 45 kDa. **c** Gene expression (determined by qRT-PCR) of *OCT4* in *foxo3* disruption mutants with or without exogenous *FOXO3*. **d** Western blot of U87MG cells with exogenous *FOXO3*. A significant difference was indicated by Student's t test compared to control U87MG cells (*) or cognate *foxo3* mutant cell line (**)

Fig. 2 *FOXO3* disruption mutants had reduced stem characteristics in U87MG cells. **a** Gene expression (for *SOX2* and *TUBB3*, encoding a neuronal marker) was determined by qRT-PCR in *foxo3* disruption mutants. Mutants had reduced *SOX2* and increased *TUBB3* expression. **b** Lysates from *foxo3* mutants and control U87MG cells were investigated by western blot analysis. Mutants had reduced STAT3 Y705 phosphorylation. **c** Indicated cancer cell lines were plated at a density of 180 cells per ml and grown for 2 weeks. Colonies were stained with crystal violet and counted. *Significant difference indicated by Students *T* test
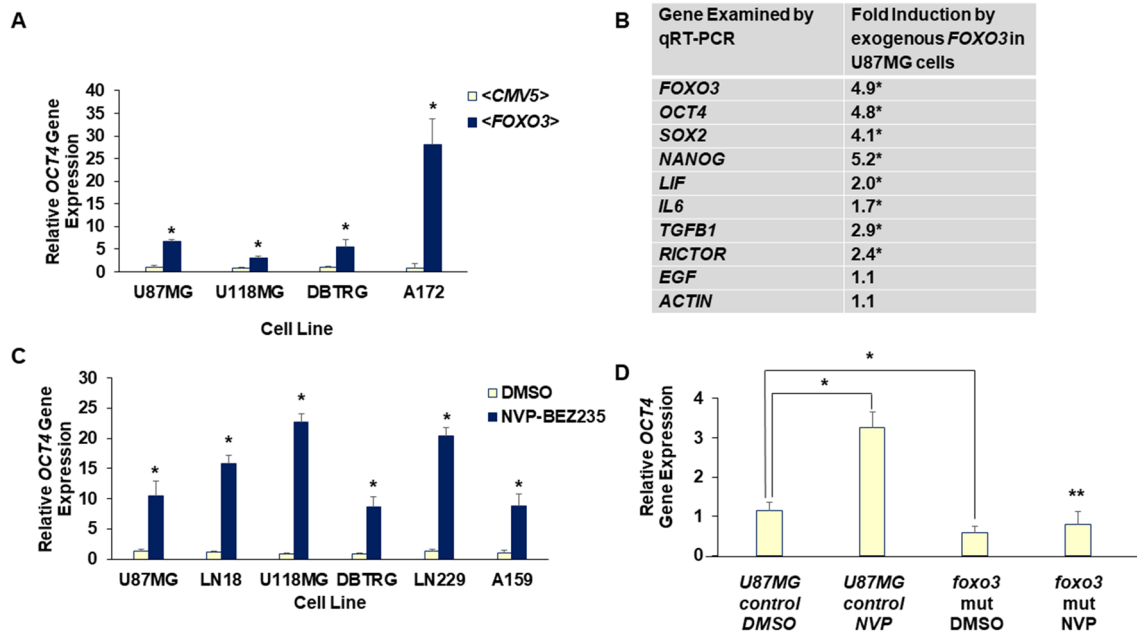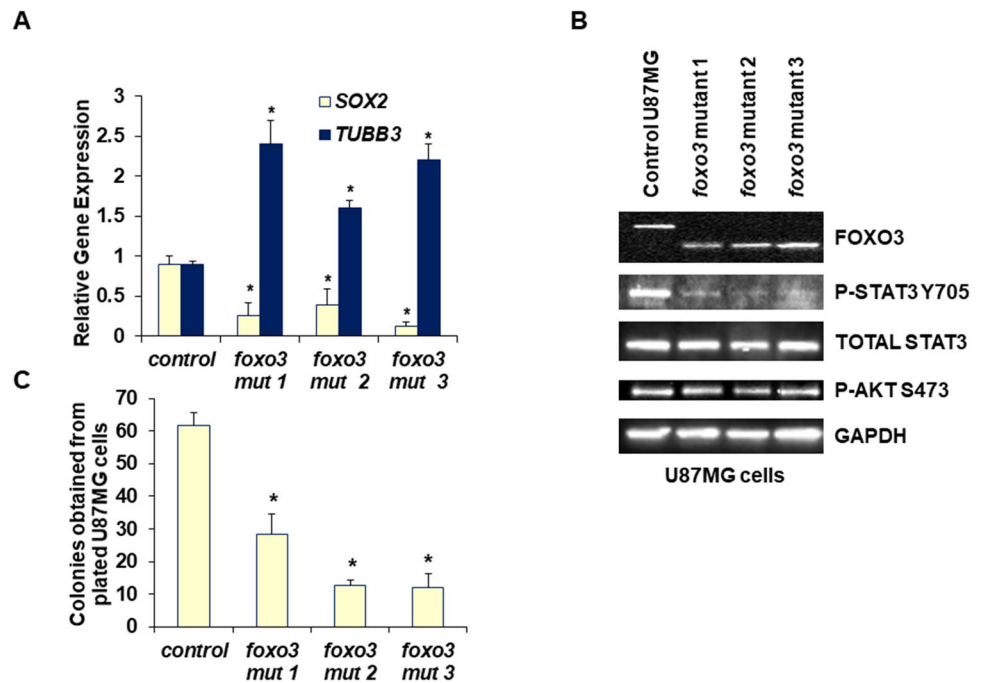
Fig. 3 Exogenous *FOXO3* and Dual PI3K Inhibitor NVP-BEZ235 Induce *OCT4*. **a** *OCT4* gene expression (determined by qRT-PCR) in four glioblastoma cell lines: U87MG, U118MG, DBTRG, and A172. **b** Expression of stem genes from samples with exogenous *FOXO3* measured by qRT-PCR. The fold induction was relative to the control samples (CMV5 vector alone). *FOXO3* and *RICTOR* were positive controls, whereas *ACTIN* (*ACTB*) was a negative control. The Benjamini–Hochberg Procedure was employed to correct for multiple hypothesis testing using an FDR < 0.05. **c** Indicated glioblastoma cell lines were treated for 5 days with NVP-BEZ235 and analyzed by qRT-PCR for *OCT4* gene expression. All cell lines were treated with 50 nM NVP-BEZ235, except LN229, which was treated with 1 μM NVP-BEZ235. **d** U87MG and *foxo3*-disrupted U87MG cells were treated with 50 nM NVP-BEZ235 for 48 h. The Tukey method was utilized for multiple comparison testing with $P < 0.05$ denoted with *. The ** denotes $P < 0.05$ based on Tukey method between U87MG NVP control cells and *foxo3* mutant treated with NVP. *Significant difference indicated by Student's *T* test in panels **a–c**
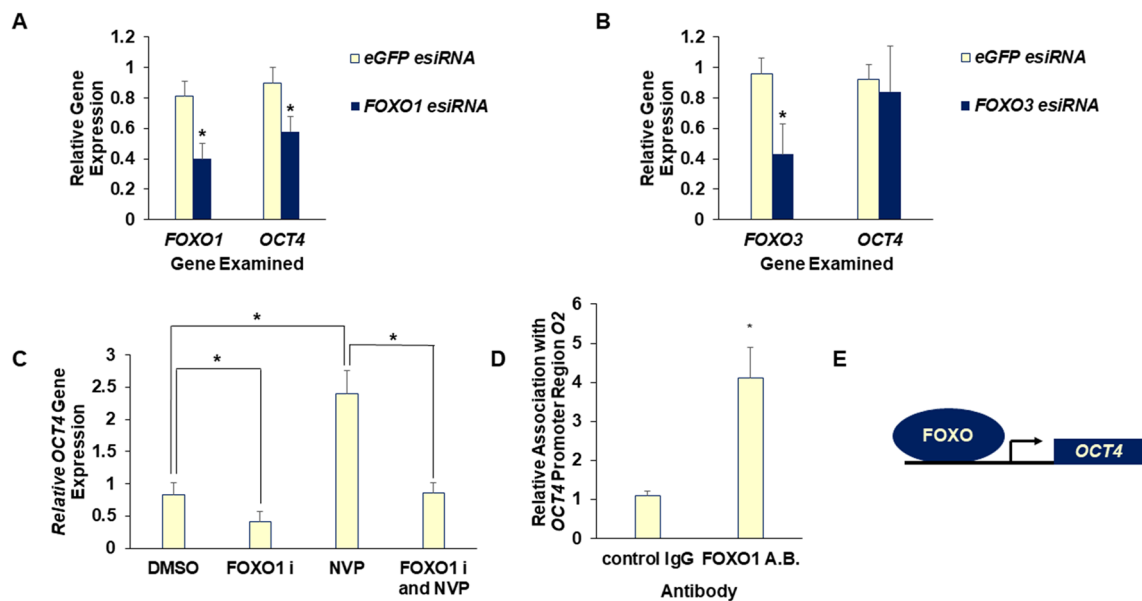
Fig. 4 FOXO1 contributes to *OCT4* gene expression in U87MG Cells. **a**, **b** Gene expression of *OCT4* or indicated FOXO factor was determined by qRT-PCR in cells with indicated esiRNA (48 h post-transfection). *FOXO1* esiRNA-treated cells had decreased *OCT4* gene expression. **c** Cells were treated with DMSO, FOXO1 inhibitor (F1i, AS1842856 200 nM), and/or NVP-BEZ235 (50 nM) for 48 h and examined by q-RT-PCR. FOXO1 inhibition led to reduced *OCT4* gene expression based on Tukey Test (*P* < 0.05), denoted by ***** in this panel. **d** ChIP was performed using extracts prepared from NVP-BEZ235 treated U87MG cells to investigate association of FOXO1 with previously mapped *OCT4* Promoter Region O2 relative to a negative control conserved upstream region of human *OCT4* (NEG Seq O). FOXO1 associated with the *OCT4* O2 promoter sequence. **e** A model is depicted in which FOXO factors directly regulate *OCT4* transcription in certain cancer cells such as U87MG GBM. *Significant difference indicated by Student's *T* test in **a**, **b**, **d**

(Figs. 1a, b) (Vazquez et al. 2018). To assess transcriptional consequences of *FOXO3* disruption in U87MG cells, we performed qRT-PCR analyses with log-phase cells grown in rich media and found significantly less *OCT4* gene expression in the mutant cells compared to control cells (Fig. 1c). Importantly, exogenous expression of *FOXO3* restored *OCT4* gene expression in the disruption mutants (Fig. 1c). Exogenous *FOXO3* also induced OCT4 protein expression in U87MG cells (Fig. 1d). These results show for the first time that FOXO3 promotes the expression of the stem master regulator *OCT4* in aggressive U87MG cells.

Loss-of-function *foxo3* mutants have reduced stem signal transduction and evidence of differentiation

To further assess the impact of *FOXO3* disruption on stem characteristics in U87MG cells, we examined expression of *SOX2*, which was shown to be impacted by FOXO factors in ES cells (Zhang et al. 2011). We found that *SOX2* gene expression was reduced in *foxo3* mutants (Fig. 2a). Interestingly, we observed an increase in *TUBB3* (*Tubulin Beta 3 class III*) expression in the disruption mutants, suggesting that these cells may have adopted a neuronal-like fate (Fig. 2a) (Poirier et al. 2010).

To investigate the impact of *FOXO3* disruption on stem signaling pathways in cancer, we examined activation of the STAT3 (signal transducer and activator of transcription 3) transcription factor. STAT3 promotes stem cell fate in part by inhibiting cellular differentiation (Raz et al. 1999). Upon IL6 or LIF ligand binding to cognate receptors, the associated Janus Kinase 2 (JAK2) phosphorylates STAT3 on tyrosine 705 thereby promoting stem gene expression (Galoczova et al. 2018; Marotta et al. 2011). We found that STAT3 Y705 phosphorylation was reduced in *foxo3* disruption mutants compared to control cells, while there was no change in total STAT3 in *foxo3* mutant cells (Fig. 2b). There was no change in AKT activation as evidenced by phosphorylation of AKT on serine 473 in the *foxo3* disruption mutants suggesting a specific impact on stem-related signal transduction by FOXO3 in this context. Therefore, *FOXO3* disruption specifically impacted STAT3 activation in U87MG cells, consistent with the idea that FOXO factors impact stem characteristics in this setting.

Clonogenicity was reduced in *foxo3* disruption mutant U87MG cells

Disruption of the *FOXO3* gene in the U87MG background gave rise to cells that appeared to have a growth defect. Clonogenicity assays were performed with *foxo3* mutants and U87MG parental controls to assess the impact of *FOXO3* disruption on colony formation. We found that disruption of

FOXO3 led to a significant decline in the number of colonies obtained (Fig. 2c), highlighting a positive role for this factor in the growth and/or survival of U87MG cells.

Exogenous *FOXO3* induced *OCT4* in a set of glioblastoma cell lines

To gain insight into the impact of *FOXO3* on stem gene expression in a set of glioblastoma cell lines, we exogenously expressed this factor (by transfection) and examined *OCT4* gene expression by qRT-PCR. We found that exogenous *FOXO3* led to increased *OCT4* gene expression in four glioblastoma cell lines: U87MG, U118MG, DBTRG, and A172 as well as human embryonic kidney cells (HEK 293) and basal breast cancer cells (BT549), Figs. 3a and S1A. Exogenous *FOXO1* also induced *OCT4* in these settings (data not shown). The ability of FOXO factors to induce the stem master regulator *OCT4* suggested that they should broadly impact stem gene expression and signal transduction. Therefore, we examined the ability of exogenous *FOXO3* to regulate additional genes encoding transcription factors ascribed to promote stem signatures as well as ligands that induce stem programs (Fig. 3b) (Galoczova et al. 2018; Loh et al. 2006; Molyneaux et al. 2003; O'Connor et al. 2008). The positive control *RICTOR* was induced by exogenous *FOXO3* whereas the negative control *ACTIN (ACTB)* was not. We found that stem transcription factors were strongly induced by exogenous *FOXO3*: *SOX2* and *NANOG* (*Nanog homeobox*) (Fig. 3b). Furthermore, exogenous *FOXO3* significantly induced the expression of stem pathway ligands *LIF* (*Leukemia Inhibitory Factor*), *IL6* (*Interleukin 6*), and *TGFB1* (*Transforming Growth Factor beta1*) whereas *EGF* (*Epidermal Growth Factor*) was not induced (Fig. 3b). These data indicate that FOXO3 broadly promoted a stem program in U87MG cancer cells potentially via the induction of the master regulator *OCT4* (Zhang et al. 2011).

Treatment with PI3K pathway inhibitor NVP-BEZ235 induced *OCT4* in glioblastoma cells

PI3K pathway activation is a hallmark of cancer and is required for the growth and survival of cancer cells (Keniry and Parsons 2008; Luo et al. 2003). In line with this, PI3K pathway inhibitors are actively explored as potential chemotherapeutics for cancer (Lin et al. 2012; Matsushima et al. 2015). To examine the impact of PI3K inhibition in cancer cells that harbor stem signatures, we treated six glioblastoma cell lines with the dual PI3K inhibitor NVP-BEZ235 (which inhibits both PI3K and mTOR) for 5 days and then examined changes in gene expression by qRT-PCR. Strikingly, we found that *OCT4* gene expression was robustly induced by NVP-BEZ235 treatment (Fig. 3c). Of note, LN229 cells required a higher dose of NVP-BEZ235 to observe

this induction (1μM compared to 50 nM). NVP-BEZ235 treatment also increased *OCT4* expression in HEK 293 and BT549 cells, demonstrating that the impact of FOXO factors on stem genes is not limited to glioblastoma cells (Fig. S1B). We also examined the gene expression of the stem marker alkaline phosphatase (encoded by *ALPP*) by qRT-PCR in NVP-BEZ235-treated samples (O'Connor et al. 2008; Yu et al. 2015, 2018). We found that PI3K inhibition led to induction of *ALPP* gene expression in U87MG, LN229, A172, and BT549 cells (Fig. S1C). Therefore, these data suggest that PI3K inhibition leads to increased stem gene expression in a set of glioblastoma cell lines. To test whether NVP-BEZ235-mediated *OCT4* induction was FOXO-dependent, we treated control and *foxo3* disruption mutants with the drug for 48 h. We found that NVP-BEZ235 only induced *OCT4* in the control U87MG cells. Cells that harbored a *foxo3* disruption mutant lacked induction of *OCT4* (Fig. 3d).

Given that the PI3K pathway is known to regulate FOXO nuclear localization, we checked whether treatment with the dual PI3K inhibitor NVP-BEZ235 impacted the localization of wild-type and/or mutant FOXO3 protein. We found that PI3K inhibition with NVP-BEZ235 alone led to less overall protein in extracts, but had no impact on FOXO3 localization in U87MG cells, consistent with findings by Zhang et al., in stem cell contexts such as ES and HSCs (Fig. S2) (Ghaffari et al. 2010; Liang et al. 2016). This is also in agreement with Sunayama et al. who found that the regulation of FOXO factor localization is complex in the glioblastoma setting of A172 cells and that inhibition with NVP-BEZ235 alone was not sufficient to direct FOXO3 to the nucleus (Sunayama et al. 2011).

Sunayama et al. found that dual inhibition of the Ras and PI3K pathways with MEK inhibitor UO126 and NVP-BEZ235, respectively, led to differentiation of glioblastoma cells A172 as evidenced by neuronal marker TUBB3 expression. In agreement with Sunayama et al., we found induction of the neuronal differentiation marker *TUBB3* upon inhibition of MEK and PI3K (Figs. S3A–B) (Sunayama et al. 2011). We also found induction of *TUBB3* with NVP-BEZ235 treatment alone in U87MG cells and concomitant induction of *OCT4* (Figs. S3A-B). Of note, the dual treatment of U87MG cells (with UO126 and NVP-BEZ235) led to significantly higher inductions of *OCT4* and *TUBB3* compared to NVP-BEZ235 treatment alone (Fig. S3A), in support of the notion that Ras and PI3K coordinately impact differentiation. All of these data highlight the dual contributions of FOXO factors and PI3K to stem cell characteristics. Loss of either FOXO (Fig. 1c) or PI3K (Figs. S3A–B) can lead to stem cell differentiation, consistent with prior reports (Daniele et al. 2015; Ghaffari et al. 2010; Ikeda and Toyoshima 2017; Jones et al. 2016; Kumazoe et al. 2017; Liang et al. 2016; Renault et al. 2009; Rivas et al. 2018).

FOXO1 contributes to *OCT4* expression in U87MG cells

We sought to determine which of the FOXO factors contributed to *OCT4* expression in U87MG cells. RNAi to *FOXO1* or *FOXO3* led to reduced expression of *OCT4* in ES cells; both of these factors directly associated with the *OCT4* promoter in ES cells based on chromatin immunoprecipitation and EMSA experiments in prior studies (Zhang et al. 2011). To examine the contributions of FOXO1 or FOXO3 on *OCT4* gene expression in U87MG cells, we transfected cells with esiRNA to target each factor independently. We found that esiRNA-mediated reduction of *FOXO1* was associated with less basal *OCT4* gene expression (Fig. 4a); NVP-BEZ235-induced *OCT4* gene expression was not significantly changed by *FOXO1* esiRNA (data not shown). Reduced *FOXO3* (via esiRNA) did not have a significant impact on *OCT4* gene expression (Fig. 4b). We also examined the ability of FOXO1 to impact *OCT4* gene expression by utilizing an FOXO1 inhibitor. Treatment of U87MG cells with FOXO1 inhibitor AS1842856 led to decreased basal and NVP-BEZ235-induced *OCT4* gene expression (Fig. 4c). Given that both FOXO1 and FOXO3 were shown to directly associate with the *OCT4* promoter in ES cells, we examined their ability to bind this promoter in extracts prepared from U87MG cells. We detected FOXO1 association with the *OCT4* promoter by quantitative chromatin immunoprecipitation analyses (Fig. 4d). Therefore, our results indicate that FOXO1 directly binds to the *OCT4* promoter and contributes to *OCT4* gene expression in U87MG cells.

Discussion

FOXO transcription factors are best known as partially redundant tumor suppressors that can induce apoptosis and halt the cell cycle (Brunet et al. 1999; Calnan and Brunet 2008). However, recent studies challenge this paradigm and point to roles for these factors in promoting cancer. *FOXO1* was found mutated to produce a constitutively nuclear protein in DLBCL, which was associated with poor prognosis (Trinh et al. 2013). Hints of pro-oncogenic roles for FOXO factors were found in additional cancers such as AML (where 40% of AML patient samples had active FOXO regardless of genetic subtype) (Sykes et al. 2011). FOXO factors hindered differentiation and apoptosis in AML cell lines and mouse models (Sykes et al. 2011). FOXO3 was shown to promote TMZ resistance in glioblastoma cells (Xu et al. 2017). Other work indicated that FOXO transcription factors were at least in part localized to the nucleus in certain PI3K-activated cancers such as BBC BT549 cells, but the function of FOXO factors in these cancers was not identified (Keniry et al. 2013). Here, we took a genetic approach to investigate the role of FOXO factors in GBM cells and found that these factors contribute to the expression of stem genes such as *OCT4*, likely contributing to the aggressiveness of these cancers (Figs. 1, 2, 3, 4).

FOXO1 and at least in part FOXO3 directly bind to and induce stem cell genes such as *OCT4* in ES cells (Zhang et al. 2011). Intriguingly, BBC and GBM commonly harbor stem cell gene expression signatures (Ben-Porath et al. 2008). We hypothesized that FOXO factors may drive stem cell signatures aggressive BBC and GBM cancer cells. In line with this notion, our results indicated that *FOXO3* disruption led to significantly reduced gene expression of *OCT4* and *SOX2* in U87MG cells, (Figs. 1, 2) and exogenous expression induced these genes in glioblastoma cell lines (Fig. 3a). Therefore, FOXO transcription factors regulate *OCT4* gene expression in glioblastoma cells (Figs. 1c–d, 2a, 3a).

OCT4 is a potent transcriptional master regulator of pluripotency. Exogenous expression of this factor is enough to instill stem-like properties to fibroblasts (Li et al. 2011). The broad impacts that *FOXO3* had on stem gene expression and signal transduction underscored a novel and exciting role for these factors in aggressive GBM (Figs. 1, 2, 3, 4). Given that FOXO factors (-1, -3, and -4) are commonly redundant, it is likely that a combination of these factors contributes to stem gene expression in U87MG cells and similar cancer settings.

Insights into FOXO3 subcellular localization and function in the setting of glioblastoma were previously described by Sunayama et al. (2011). In Sunayama et al., FOXO3 contributed to differentiation upon PI3K and Ras inhibition in glioblastoma cells. We performed similar experiments and found increased expression of *TUBB3* in PI3K/Ras inhibited U87MG cells, in agreement with Sunayama et al. (Fig. S3A–B). Of note, we found increased *TUBB3* gene expression in U87MG cells that were only treated with NVP-BEZ235 (Fig. S3A–B). One possibility is that Ras might not have been as activated in U87MG cells; therefore, inhibition of NVP-BEZ235 alone may have been enough to induce differentiation. We detected induction of both differentiation and stem genes under NVP-BEZ235 treatment in U87MG cells (Figs. S3A–B). Intriguingly, we do not know yet whether the same cells express stem and differentiation genes, or distinct populations express these genes.

There was one slight difference between our work and Sunayama et al.; we found that *FOXO3* disruption led to increased *TUBB3* (Fig. 2a), whereas Sunayama et al. found that cells with decreased *FOXO3* by siRNA had reduced *TUBB3* gene expression. One possible explanation for this discrepancy is that *FOXO3* disruption led to a loss in stem characteristics and differentiation (including *TUBB3* induction) over a period of weeks in our experiments compared to three days for Sunayama et al. (2011). It is noteworthy that although FOXO3 protein was nearly undetectable after

RNAi targeting in work by Sunayama et al., *TUBB3* was still induced, albeit at a reduced level. This suggests that other FOXO factors may have contributed to *TUBB3* expression in these experiments. Similarly, in our experiments, other factors may have promoted *TUBB3* induction (such as FOXO1) when *FOXO3* was disrupted.

Our results from subcellular localization experiments for FOXO factors matched Sunayama et al. (2011). Treatment with NVP-BEZ235 alone did not appreciably change FOXO3 (wild-type or disruption mutant) subcellular localization, refining conventional paradigms for this pathway (Fig. S2). FOXO1 and FOXO4 localization was not impacted by NVP-BEZ235 treatment of U87MG cells (data not shown). Even though the localization of FOXO factors were unchanged by NVP-BEZ235 treatment, it appeared that target genes were induced (Figs. 3c and S2A).

Other studies have highlighted the ability of NVP-BEZ235 to induce FOXO output in cancer cells. Lin et al. examined feedback responses under low-dose NVP-BEZ235 conditions (Lin et al. 2014). One key point from Lin et al. was that the FOXO-dependent resurgence of PI3K activity was only observed at a relatively low dose of NVP-BEZ235 (Lin et al. 2014). Lin et al. specifically chose to use a low dose of NVP-BEZ235, because higher dosages would likely be toxic to cancer patients. Our work built on the work by Lin et al. In addition to deleterious effects mediated by FOXO that led to PI3K pathway reactivation (*RICTOR* induction, Fig. 3b), NVP-BEZ235 treatment had additional deleterious effects that could greatly impact drug efficacy as a chemotherapeutic. We found that stem genes were induced upon NVP-BEZ235 treatment (Figs. 3c and S1B-C). Our experiments mostly employed low dosage NVP-BEZ235 (similar to experiments performed by Lin et al.). Two sets of our experiments utilized higher doses of NVP-BEZ235. We needed to use a higher dose of NVP-BEZ235 to observe stem gene induction in the glioblastoma cell line LN229 (1 μM compared to 50 nM for other cell lines, Fig. 3c). Perhaps, the PI3K pathway is more active in LN229 cells. We also utilized a higher NVP-BEZ235 dose (1 μM) when examining subcellular localization to compare our work to Sunayama et al. (who utilized 1 μM) as well as to examine changes in gene expression with combined MEK and PI3K inhibition (Lin et al. 2014; Sunayama et al. 2011).

Targeting PI3K as a chemotherapeutic for cancer requires consideration of homeostatic feedback mechanisms and possible unwanted activation of pathways that may promote cancer aggressiveness. The efficacy of PI3K targeted therapy for advanced solid tumors was limited and did not significantly increase overall survival or objective response rate across 46 randomized-controlled clinical trials (Li et al. 2018). Work by Caino et al., demonstrated that PI3K pathway inhibition led to increased cellular motility in prostate cancer cells as well as reactivation of PI3K signal transduction (Caino et al. 2015). Hopkins et al. mitigated the homeostatic feedback mechanisms induced by PI3K inhibition by utilizing a ketogenic diet in a murine pancreatic cancer model, highlighting novel avenues that show promise for future therapeutic protocols (Hopkins et al. 2018). Our work has novel implications for transcriptional changes that arise upon PI3K inhibition. We found PI3K inhibition by NVP-BEZ235 led to the robust induction of stem genes such as *OCT4* in a set of glioblastoma cell lines and BT549 cells. It remains unclear if PI3K inhibition will broadly induce stem programs across varied subtypes of cancer or if it will only be pertinent to the most aggressive cancers that already harbor stem signatures such as glioblastoma cells and BT549.

Conclusions

FOXO transcription factors function in a context-dependent manner (Paik et al. 2007). In some cancers, FOXO factors cause apoptosis (Calnan and Brunet 2008). We found that FOXO factors promote stem gene expression in GBM cells (Figs. 1, 2, 3, 4). Treatment with the dual PI3K inhibitor NVP-BEZ235 induced stem gene expression in glioblastoma cell lines and BT549 cells (Fig. 2c, d), having important implications for the efficacy of PI3K inhibition as a chemotherapeutic option. Importantly, expression of stem programs is strongly associated with poor prognosis, suggesting that PI3K inhibition may make some susceptible cancers more aggressive (Iwadate et al. 2017). Perhaps combined PI3K pathway and FOXO inhibition would be more efficacious as a cancer therapy, because it would target proliferation and residual stem cells.

Methods

Cell culture and drug treatments

Cell lines were obtained from ATCC (American Type Culture Collection, Manassas, VA) and grown under standard conditions (5% CO_2, 10% FBS (fetal bovine serum), with 5% antifungal/antibacterial). Cell lines were tested for Mycoplasma using the MycoAlert Mycoplasma Detection Kit (Lonza, Basel Switzerland, cat: LT07-218); all experiments were done with mycoplasma negative cells. U87MG cells were propagated in MEM (Minimal Essential Medium). BT549 and DBTRG cells were propagated in RPMI (Roswell Park Memorial Institute 1640 Medium). HEK 293, LN18, U118MG, A172, and LN229 cells were propagated in DMEM (Dulbecco's Modified Eagle Medium). NVP-*BEZ235* was purchased from Sigma (Saint Louis, MO), and utilized at a final concentration of 50 nM in indicated experiments. Two sets of experiments utilized a higher

dose of NVP-BEZ235. LN229 cells were treated with 1 μM NVP-BEZ235 and data from Figs. S3A–B were generated using 1 μM NVP-BEZ235 treatment. UO126 was purchased from Selleck Chemicals (Houston, TX) and used at 10 μM final concentration. Cells were plated at a density of 2700 cells per ml and were treated for 5 days with NVP-BEZ235 (unless otherwise stated). AS1842856 was purchased from Calbiochem (Danvers, MA) and utilized at 200 nM final concentration.

Transfection

Cells were grown under standard propagating conditions (37 °C with 5% CO_2 in media containing 10% FBS and 5% pen/strep) and harvested by trypsin treatment, while the cells were in the log growth phase. One million cells were transfected using Lonza Nucleofection kit V (Lonza, Basel Switzerland), program P-20 (U87MG, A172, LN229, LN18, U118, DBTRG, and BT549) or X-001 (HEK 293) and allowed to recover for 24 h in 10 cm culture dishes. The *foxo3* disruption mutants and controls were electroporated using program T-020 with Lonza Nucleofection kit V and 1 million cells. One microgram of indicated plasmid was utilized in each transfection. Plasmids were described previously (Keniry et al. 2013). *FOXO3*-CMV5 was obtained from D. Accili (Nakae et al. 2001). Vectors prepared for CRISPR Cas9 mutagenesis were previously described (Vazquez et al. 2018). The CRISPR donor vector was prepared using a pCDNA3 backbone with chromosomal *FOXO3* sequences to enable integration into *FOXO3* loci to disrupt *FOXO3* with a *NPTII* neomycin resistance cassette. Isolates were previously confirmed by sequencing and western blot (Vazquez et al. 2018). RNAi experiments utilized Lonza Nucleofection kit V and 1 million cells with 600 ng of indicated esiRNAs from Sigma per transfection (eGFP: EHUE-GFP), (*FOXO1*: EHU156591) and (*FOXO3*: EHU113611). RNAi lysates were collected 48 h post-transfection.

Western blot

Total protein was obtained from indicated cells by rinsing cells with 1XPBS (phosphate-buffered saline) followed by directed lysis in 2 × sample buffer (125 mM Tris–HCL at pH 6.8, 2% sodium dodecyl sulfate (SDS), 10% 2-mercaptoethanol, 20% glycerol, 0.05% bromophenol blue, 8 M urea); 2 × sample buffer was added to each well and cells scraped with a cell scraper. The lysate was collected from each well, placed into 1.5 ml microcentrifuge tubes, and heated for 10 min at 95 °C in a dry-bath heat block. Protein lysates were separated by sodium dodecyl sulfate–polyacrylamide gel electrophoresis (SDS-PAGE) at 100 V for 1 h. Resolved proteins were then transferred onto a polyvinylidene fluoride (PVDF) membrane for an hour and 30 min then blocked

in a 5% milk solution (Carnation powdered milk, 1X Tris-buffered saline with Tween 20 (TBST) for an hour. Membranes were incubated with indicated primary antibody overnight at 4 °C then washed for 20 min with TBST in 5-min intervals. The blot was then incubated with secondary antibody for 1.5 h. Membranes were washed for 20 min in 5-min intervals and allowed to develop using SuperSignal West Dura Extended Duration Substrate luminol solution (Pierce Biotechnology, Waltham, MA) for 5 min. A Bio Rad ChemDoc XRS + Molecular Imager was utilized for protein detection (Bio Rad Hercules, CA). Data were analyzed with NIH Image J. Antibodies were obtained from Cell Signaling Technologies (Danvers, MA): FOXO3 (75D8), FOXO1 (C29H4), FOXO4 (9472S), OCT4 (2750S), total STAT3 (9139 T), phospho STAT3 tyrosine 705 (9145 T), and Phospho-p44/42 MAPK (Erk1/2) (Thr202/Tyr204) (D13.14.4E) XP® Rabbit mAb catalog: 4370), Histone H3 (96C10, catalog: 3638), and phospho AKT serine 473 (9271S). Antibodies obtained from Cell Signaling Technologies were diluted 1:1000 in TBST containing 5% BSA and were incubated with blots overnight at 4 °C. GAPDH (G-9) was obtained from Santa Cruz Biotechnology Inc. (Dallas, TX) and utilized at a 1:2000 dilution in TBST with 5% non-fat dried milk. Beta-Actin antibody (clone AC-74, cat: A2228) was obtained from Sigma and utilized at a 1:2000 dilution in TBST with 5% non-fat dried milk.

Quantitative real-time PCR

Total RNA was prepared using the Qiagen RNeasy kit (Hilden, Germany), which was then used to generate cDNA using Superscript Reverse Transcriptase II (Invitrogen, Carlsbad, CA). Samples (cDNAs) were analyzed using (Power SYBR Green Master Mix, Applied Biosystems, Foster City, CA) and the Illumina Eco Real-time system (San Diego, CA). Expression levels were normalized to *GAPDH* in gene expression experiments and calculated using $2^{-\Delta\Delta CT}$ method (Livak and Schmittgen 2001). Primer sequences are detailed in supplemental Table S1.

Clonogenicity assays

Indicated cells were treated with trypsin and counted using a Millipore Scepter automated cell counter (Millipore, Burlington, MA). Cells were diluted into media at a final concentration of 180 cells per ml. 2 ml of cells were plated per well of a 6-well plate and were grown for 2 weeks. Colonies were stained with 0.5% crystal violet in buffered formalin and washed with PBS. All visible colonies were counted for each sample irrespective of the cell number. Experiments were performed several times in quadruplicate.

ChIP analyses

Data presented were from U87MG cells treated with 50 nM NVP-BEZ235 for 5 days. Chromatin immunoprecipitation (ChIP) analyses were performed as previously described (Niu et al. 2003), except an additional micrococcal nuclease step was added to shear chromatin. 10 million U87MG cells grown in 15 cm dishes were cross-linked by adding formaldehyde to final concentration of 1% and incubated in room temperature for 10 min; after, 125 mM glycine was added and samples were incubated for an additional 5 min at room temperature. Cells were washed twice with PBS and scraped into ice-cold PBS, and then collected by centrifugation at $200 \times g$. Cells were washed with PBS and resuspended in ChIP lysis buffer (1% SDS, 1 mM EDTA, 50 mM Tris–HCl pH 7.5.0) Cells were lysed for 10 min on ice, sonicated on a Branson 250 Sonicator at 20% power for 30 s 4 times. After this, 18 µl of micrococcal nuclease solution (Thermo-Fisher Waltham MA, catalog: 88216) and 430 µl of 10 mM $CaCl_2$ were added to 10 ml chromatin mixture and incubated for 10 min. The reaction was stopped by adding 100 µl of 0.5 M EDTA. Next, chromatin preps were diluted 1–10 with dilution buffer (20 mM Tris–HCl pH 8.0, 1 mM EDTA, 0.1% sodium deoxycholate, 140 mM NaCl, 0.01% SDS, and 1% NP40). Chromatin was pre-cleared with 80 µl of magnetic protein A/G beads (Pierce Biotechnology, Waltham, MA, catalog: 78609) for 1 h at 4 °C. Pre-cleared chromatin preparations (prepared from 1 million cells) were incubated overnight with 7 µg of normal rabbit IgG (Santa Cruz Biotechnology Inc., Dallas, TX, catalog: SC2017) or FOXO1 antibody (C29H4) at 4 °C. Samples were next incubated with 80 µl of Protein A/G agarose for 1 h and then washed for 5 min with each buffer: Low Salt Buffer (20 mM Tris pH 8.0, 2 mM EDTA, 0.1% SDS, 1% Triton X100, and 150 mM NaCl), High Salt Buffer (20 mM Tris pH 8.0, 2 mM EDTA, 0.1% SDS, 1% Triton X100, and 500 mM NaCl), and LiCl Buffer (20mMTris pH 8.0, 2 mM EDTA, 0.5% sodium deoxycholate, 0.1% NP40, and 250 mM LiCl). After washes, DNA was eluted by incubating beads with Elution buffer (1% SDS, 0.1 M $NaHCO_3$) at 37 °C for 15 min (step performed twice). Crosslinks were reversed by adding 40 µl 2.5 M NaCl to the combined eluates (500 µl) and heating at 65 °C overnight. DNA was purified using phenol:chloroform extraction and sodium acetate/ethanol precipitation. The purified DNA was subjected to quantitative real-time PCR. *OCT4* promoter sequence O2 association levels (mapped by Zhang et al.) were normalized to *OCT4* control sequence (utilized by Zhang et al.) in ChIP experiments and calculated using $2^{-\Delta\Delta CT}$ method (Livak and Schmittgen 2001; Zhang et al. 2011). Primer sequences utilized for ChIP quantitative PCR are detailed in supplemental Table S2.

Subcellular fractionations

Subcellular fractionations were prepared as described previously (Keniry et al. 2013). 10 million log-phase cells were scraped from 15 cm plates into ice-cold PBS. Cells were washed once with ice-cold PBS (containing $1 \times$ PI). Cells were incubated in Buffer A (10 mM Hepes pH 7.4, 10 mM KCL, 100 µM EDTA, 1 X PI) for 15 min on ice. After this, 10% NP-40 was added to the Buffer A mixture at a 1:20 dilution. Samples were vortexed and incubated on ice for 2 min with mixing by inversion every 30 s. Next, samples were centrifuged at $1000 \times g$ for 5 min. The cytoplasmic fractions were collected from the supernatant and mixed one to one with $2 \times$ sample buffer (125 mM Tris–HCL at pH 6.8, 2% sodium dodecyl sulfate (SDS), 10% 2-mercaptoethanol, 20% glycerol, 0.05% bromophenol blue, and 8 M urea). Cytoplasmic fractions (mixed with $2 \times$ sample buffer) were heated for 10 min at 95 °C in a dry-bath heat block. The nuclear pellets (from the $1000 \times g$ centrifugation step) were washed with Buffer A and then washed with Buffer C (20 mM Hepes pH 7.4, 400 mM NaCl, 1 mM EDTA, 1 X PI). The washed nuclear pellets were lysed in $2 \times$ sample buffer and heated for 10 min at 95 °C in a dry-bath heat block. Samples were analyzed by western blot analyses. 25% of each nuclear fraction was resolved in each well for western blot analyses. 1% of each cytoplasmic fraction was resolved in each well for western blot analyses. Experiments were repeated several times with similar results.

Compliance with ethical standards

Conflict of interest The authors declare that they have no competing interests.

Ethics approval Work was performed with Institutional Biosafety Committee approval from the University of Texas Rio Grande Valley: Registration number: 2016–003-IBC.

References

Bellacosa A et al (1998) Akt activation by growth factors is a multiple-step process: the role of the PH domain. Oncogene 17:313–325. https://doi.org/10.1038/sj.onc.1201947

Ben-Porath I, Thomson MW, Carey VJ, Ge R, Bell GW, Regev A, Weinberg RA (2008) An embryonic stem cell-like gene expression signature in poorly differentiated aggressive human tumors. Nat Genet 40:499–507. https://doi.org/10.1038/ng.127

Bigarella CL, Li J, Rimmele P, Liang R, Sobol RW, Ghaffari S (2017) FOXO3 transcription factor is essential for protecting hematopoietic stem and progenitor cells from oxidative DNA damage. J Biol Chem 292:3005–3015. https://doi.org/10.1074/jbc.M116.769455

Brunet A et al (1999) Akt promotes cell survival by phosphorylating and inhibiting a Forkhead transcription factor. Cell 96:857–868

Caino MC et al (2015) PI3K therapy reprograms mitochondrial trafficking to fuel tumor cell invasion. Proc Natl Acad Sci USA 112:8638–8643. https://doi.org/10.1073/pnas.1500722112

Calnan DR, Brunet A (2008) The FoxO code Oncogene 27:2276–2288. https://doi.org/10.1038/onc.2008.21

Daniele S et al (2015) Combined inhibition of AKT/mTOR and MDM2 enhances Glioblastoma Multiforme cell apoptosis and differentiation of cancer stem cells. Sci Rep 5:9956. https://doi.org/10.1038/srep09956

Galoczova M, Coates P, Vojtesek B (2018) STAT3, stem cells, cancer stem cells and p63. Cell Mol Biol Lett 23:12. https://doi.org/10.1186/s11658-018-0078-0

Ghaffari SG et al (2010) Foxo1 is essential for the regulation of pluripotency in embryonic stem cells. Exp Hematol 38:S120–S120

Hagenbuchner J et al (2016) Nuclear FOXO3 predicts adverse clinical outcome and promotes tumor angiogenesis in neuroblastoma. Oncotarget 7:77591–77606. https://doi.org/10.18632/oncotarget.12728

Hopkins BD et al (2018) Suppression of insulin feedback enhances the efficacy of PI3K inhibitors. Nature 560:499–503. https://doi.org/10.1038/s41586-018-0343-4

Ikeda M, Toyoshima F (2017) Dormant pluripotent cells emerge during neural differentiation of embryonic stem cells in a FoxO3-dependent manner. Mol Cell Biol. https://doi.org/10.1128/MCB.00417-16

Iwadate Y et al (2017) The pluripotent stem-cell marker alkaline phosphatase is highly expressed in refractory glioblastoma with DNA hypomethylation. Neurosurgery 80:248–256. https://doi.org/10.1093/neuros/nyw026

Jacobs FM, van der Heide LP, Wijchers PJ, Burbach JP, Hoekman MF, Smidt MP (2003) FoxO6, a novel member of the FoxO class of transcription factors with distinct shuttling dynamics. J Biol Chem 278:35959–35967. https://doi.org/10.1074/jbc.M302804200

Jones NM, Rowe MR, Shepherd PR, McConnell MJ (2016) Targeted inhibition of dominant PI3-kinase catalytic isoforms increase expression of stem cell genes in glioblastoma cancer stem cell models. Int J Oncol 49:207–216. https://doi.org/10.3892/ijo.2016.3510

Keniry M et al (2013) Survival factor NFIL3 restricts FOXO-induced gene expression in cancer. Genes Dev 27:916–927. https://doi.org/10.1101/gad.214049.113

Keniry M, Parsons R (2008) The role of PTEN signaling perturbations in cancer and in targeted therapy. Oncogene 27:5477–5485. https://doi.org/10.1038/onc.2008.248

Kumazoe M et al (2017) The FOXO3/PGC-1beta signaling axis is essential for cancer stem cell properties of pancreatic ductal adenocarcinoma. J Biol Chem 292:10813–10823. https://doi.org/10.1074/jbc.M116.772111

Li J et al (1997) PTEN, a putative protein tyrosine phosphatase gene mutated in human brain, breast, and prostate cancer. Science 275:1943–1947

Li Y et al (2011) Generation of iPSCs from mouse fibroblasts with a single gene, Oct4, and small molecules. Cell Res 21:196–204. https://doi.org/10.1038/cr.2010.142

Li X, Dai D, Chen B, Tang H, Xie X, Wei W (2018) Efficacy of PI3K/AKT/mTOR pathway inhibitors for the treatment of advanced solid cancers: a literature-based meta-analysis of 46 randomised control trials. PLoS ONE 13:e0192464. https://doi.org/10.1371/journal.pone.0192464

Liang R, Rimmele P, Bigarella CL, Yalcin S, Ghaffari S (2016) Evidence for AKT-independent regulation of FOXO1 and FOXO3 in haematopoietic stem and progenitor cells. Cell Cycle 15:861–867. https://doi.org/10.1080/15384101.2015.1123355

Lin SF, Huang YY, Lin JD, Chou TC, Hsueh C, Wong RJ (2012) Utility of a PI3K/mTOR inhibitor (NVP-BEZ235) for thyroid cancer therapy. PLoS ONE 7:e46726. https://doi.org/10.1371/journal.pone.0046726

Lin A, Piao HL, Zhuang L, dos Sarbassov D, Ma L, Gan B (2014) FoxO transcription factors promote AKT Ser473 phosphorylation and renal tumor growth in response to pharmacologic inhibition of the PI3K-AKT pathway. Cancer Res 74:1682–1693. https://doi.org/10.1158/0008-5472.CAN-13-1729

Livak KJ, Schmittgen TD (2001) Analysis of relative gene expression data using real-time quantitative PCR and the 2(-Delta Delta C(T)). Method Methods 25:402–408. https://doi.org/10.1006/meth.2001.1262

Loh YH et al (2006) The Oct4 and Nanog transcription network regulates pluripotency in mouse embryonic stem cells. Nat Genet 38:431–440. https://doi.org/10.1038/ng1760

Luo J, Manning BD, Cantley LC (2003) Targeting the PI3K-Akt pathway in human cancer: rationale and promise. Cancer Cell 4:257–262

Manning BD, Cantley LC (2007) AKT/PKB signaling: navigating downstream. Cell 129:1261–1274. https://doi.org/10.1016/j.cell.2007.06.009

Marotta LL et al (2011) The JAK2/STAT3 signaling pathway is required for growth of CD44(+)CD24(-) stem cell-like breast cancer cells in human tumors. J Clin Invest 121:2723–2735. https://doi.org/10.1172/JCI44745

Matsushima M et al (2015) Intravesical dual PI3K/mTOR complex 1/2 inhibitor NVP-BEZ235 therapy in an orthotopic bladder cancer model. Int J Oncol 47:377–383. https://doi.org/10.3892/ijo.2015.2995

Miyamoto K et al (2007) Foxo3a is essential for maintenance of the hematopoietic stem cell pool. Cell Stem Cell 1:101–112. https://doi.org/10.1016/j.stem.2007.02.001

Molyneaux KA, Schaible K, Wylie C (2003) GP130, the shared receptor for the LIF/IL6 cytokine family in the mouse, is not required for early germ cell differentiation, but is required cell-autonomously in oocytes for ovulation. Development 130:4287–4294

Nakae J, Kitamura T, Silver DL, Accili D (2001) The forkhead transcription factor Foxo1 (Fkhr) confers insulin sensitivity onto glucose-6-phosphatase expression. J Clin Invest 108:1359–1367. https://doi.org/10.1172/JCI12876

Niu H, Cattoretti G, Dalla-Favera R (2003) BCL6 controls the expression of the B7–1/CD80 costimulatory receptor in germinal center B cells. J Exp Med 198:211–221. https://doi.org/10.1084/jem.20021395

O'Connor MD et al (2008) Alkaline phosphatase-positive colony formation is a sensitive, specific, and quantitative indicator of undifferentiated human embryonic stem cells. Stem Cells 26:1109–1116. https://doi.org/10.1634/stemcells.2007-0801

Oh HM, Yu CR, Dambuza I, Marrero B, Egwuagu CE (2012) STAT3 protein interacts with Class O Forkhead transcription factors in the cytoplasm and regulates nuclear/cytoplasmic localization of FoxO1 and FoxO3a proteins in CD4(+) T cells. J Biol Chem 287:30436–30443. https://doi.org/10.1074/jbc.M112.359661

Okkenhaug K, Vanhaesebroeck B (2003) PI3K in lymphocyte development, differentiation and activation. Nat Rev Immunol 3:317–330. https://doi.org/10.1038/nri1056

Paik JH et al (2007) FoxOs are lineage-restricted redundant tumor suppressors and regulate endothelial cell homeostasis. Cell 128:309–323. https://doi.org/10.1016/j.cell.2006.12.029

Poirier K et al (2010) Mutations in the neuronal ss-tubulin subunit TUBB3 result in malformation of cortical development and neuronal migration defects. Hum Mol Genet 19:4462–4473. https://doi.org/10.1093/hmg/ddq377

Raz R, Lee CK, Cannizzaro LA, d'Eustachio P, Levy DE (1999) Essential role of STAT3 for embryonic stem cell pluripotency. Proc Natl Acad Sci USA 96:2846–2851

Renault VM et al (2009) FoxO3 regulates neural stem cell homeostasis. Cell Stem Cell 5:527–539. https://doi.org/10.1016/j.stem.2009.09.014

Rivas S, Gomez-Oro C, Anton IM, Wandosell F (2018) Role of Akt isoforms controlling cancer stem cell survival. Phenotype Self Renew Biomed. https://doi.org/10.3390/biomedicines6010029

Saal LH et al (2005) PIK3CA mutations correlate with hormone receptors, node metastasis, and ERBB2, and are mutually exclusive with PTEN loss in human breast carcinoma. Cancer Res 65:2554–2559. https://doi.org/10.1158/0008-5472-CAN-04-3913

Saal LH et al (2007) Poor prognosis in carcinoma is associated with a gene expression signature of aberrant PTEN tumor suppressor pathway activity. Proc Natl Acad Sci USA 104:7564–7569. https://doi.org/10.1073/pnas.0702507104

Saal LH et al (2008) Recurrent gross mutations of the PTEN tumor suppressor gene in breast cancers with deficient DSB repair. Nat Genet 40:102–107. https://doi.org/10.1038/ng.2007.39

Sunayama J et al (2011) FoxO3a functions as a key integrator of cellular signals that control glioblastoma stem-like cell differentiation and tumorigenicity. Stem Cells 29:1327–1337. https://doi.org/10.1002/stem.696

Sykes SM et al (2011) AKT/FOXO signaling enforces reversible differentiation blockade in myeloid leukemias. Cell 146:697–708. https://doi.org/10.1016/j.cell.2011.07.032

Tothova Z, Gilliland DG (2007) FoxO transcription factors and stem cell homeostasis: insights from the hematopoietic system. Cell Stem Cell 1:140–152. https://doi.org/10.1016/j.stem.2007.07.017

Tothova Z et al (2007) FoxOs are critical mediators of hematopoietic stem cell resistance to physiologic oxidative stress. Cell 128:325–339. https://doi.org/10.1016/j.cell.2007.01.003

Trinh DL et al (2013) Analysis of FOXO1 mutations in diffuse large B-cell lymphoma. Blood 121:3666–3674. https://doi.org/10.1182/blood-2013-01-479865

van der Heide LP, Jacobs FM, Burbach JP, Hoekman MF, Smidt MP (2005) FoxO6 transcriptional activity is regulated by Thr26 and Ser184, independent of nucleo-cytoplasmic shuttling. Biochem J 391:623–629. https://doi.org/10.1042/BJ20050525

Vazquez N et al (2018) A protocol for custom CRISPR Cas9 donor vector construction to truncate genes in mammalian cells using pcDNA3 backbone. BMC Mol Biol 19:3. https://doi.org/10.1186/s12867-018-0105-8

Xu K, Zhang Z, Pei H, Wang H, Li L, Xia Q (2017) FoxO3a induces temozolomide resistance in glioblastoma cells via the regulation of beta-catenin nuclear accumulation. Oncol Rep 37:2391–2397. https://doi.org/10.3892/or.2017.5459

Yu Z et al (2015) Differential properties of human ALP(+) periodontal ligament stem cells vs their ALP(-) counterparts. J Stem Cell Res Ther. https://doi.org/10.4172/2157-7633.1000292

Yu F et al (2018) FoxO1 inhibition promotes differentiation of human embryonic stem cells into insulin producing cells. Exp Cell Res 362:227–234. https://doi.org/10.1016/j.yexcr.2017.11.022

Zhang X et al (2011) FOXO1 is an essential regulator of pluripotency in human embryonic stem cells. Nat Cell Biol 13:1092–1099. https://doi.org/10.1038/ncb2293

Publisher's Note Springer Nature remains neutral with regard to jurisdictional claims in published maps and institutional affiliations.